Digital generation of shape-invariant Bessel-like beams

Igor A. Litvin,[1,*] Thandeka Mhlanga,[1] and Andrew Forbes[1,2]

[1]*CSIR National Laser Centre, PO Box 395, Pretoria 0001, South Africa*
[2]*School of Physics, University of the Witwatersrand, Johannesburg 2050, South Africa*
[*]*ILitvin@csir.co.za*

Abstract: Bessel beams have been extensive studied to date but are always created over a finite region inside the laboratory. Means to overcome this consider multi-element refractive designs to create beams that have a longitudinal dependent cone angle, thereby allowing for a far greater quasi non–diffracting propagation region. Here we outline a generalized approach for the creation of shape-invariant Bessel-like beams with a single phase-only element, and demonstrate it experimentally with a phase-only spatial light modulator. Our experimental results are in excellent agreement with theory, suggesting an easy-to-implement approach for long range, shape-invariant Bessel-like beams.

OCIS codes: (140.3295) Laser beam characterization; (140.3300) Laser beam shaping; (350.5500) Propagation; (050.1940) Diffraction.

References and links

1. J. Durnin, "Exact solutions for nondiffracting beams. The scalar theory," J. Opt. Soc. Am. B **4**(4), 651 (1987).
2. J. Durnin, J. J. Miceli, Jr., and J. H. Eberly, "Diffraction-free beams," Phys. Rev. Lett. **58**(15), 1499–1501 (1987).
3. D. McGloin and K. Dholakia, "Bessel beams: diffraction in a new light," Contemp. Phys. **46**(1), 15–28 (2005).
4. M. Mazilu, D. J. Stevenson, F. Gunn-Moore, and K. Dholakia, "Light beats the spread: non-diffracting beams," Laser Photon. Rev. **4**(4), 529–547 (2010).
5. A. Dudley, M. Lavery, M. J. Padgett, and A. Forbes, "Unraveling Bessel beams," Opt. Photonics News **24**(6), 22–29 (2013).
6. A. N. Khilo, E. G. Katranji, and A. A. Ryzhevich, "Axicon-based Bessel resonator: Analytical description and experiment," J. Opt. Soc. Am. A **18**(8), 1986–1992 (2001).
7. J. Rogel-Salazar, G. H. C. New, and S. Chavez-Cerda, "Bessel-Gauss beam optical resonator," Opt. Commun. **190**(1-6), 117–122 (2001).
8. I. A. Litvin and A. Forbes, "Bessel–Gauss resonator with internal amplitude filter," Opt. Commun. **281**(9), 2385–2392 (2008).
9. R. Vasilyeu, A. Dudley, N. Khilo, and A. Forbes, "Generating superpositions of higher-order Bessel beams," Opt. Express **17**(26), 23389–23395 (2009).
10. A. Vasara, J. Turunen, and A. T. Friberg, "Realization of general nondiffracting beams with computer-generated holograms," J. Opt. Soc. Am. A **6**(11), 1748–1754 (1989).
11. C. Paterson and R. Smith, "Higher-order Bessel waves produced by axicon-type computer-generated holograms," Opt. Commun. **124**(1-2), 121–130 (1996).
12. R. Bowman, N. Muller, X. Zambrana-Puyalto, O. Jedrikiewicz, P. Di Tramapani, and M. J. Padgett, "Efficient generation of Bessel beam arrays by means of an SLM," Eur. Phys. J. Spec. Top. **199**(1), 159–166 (2011).
13. N. Chattrapiban, E. A. Rogers, D. Cofield, W. T. Hill 3rd, and R. Roy, "Generation of nondiffracting Bessel beams by use of a spatial light modulator," Opt. Lett. **28**(22), 2183–2185 (2003).
14. J. Turunen, A. Vasara, and A. T. Friberg, "Holographic generation of diffraction-free beams," Appl. Opt. **27**(19), 3959–3962 (1988).
15. M. Bock, S. K. Das, and R. Grunwald, "Programmable ultrashort-pulsed flying images," Opt. Express **17**(9), 7465–7478 (2009).
16. M. McLaren, T. Mhlanga, M. J. Padgett, F. S. Roux, and A. Forbes, "Self-healing of quantum entanglement after an obstruction," Nat. Commun. **5**, 3248 (2014).
17. M. McLaren, M. Agnew, J. Leach, F. S. Roux, M. J. Padgett, R. W. Boyd, and A. Forbes, "Entangled Bessel-Gaussian beams," Opt. Express **20**(21), 23589–23597 (2012).
18. H. C. Ramrez, R. R. Alarcon, F. J. Morelos, P. A. Q. Su, J. C. G. Vega, and A. B. U'Ren, "Observation of non-diffracting behavior at the single-photon level," Opt. Express **20**(28), 29761–29768 (2012).

#227141 - $15.00 USD Received 19 Nov 2014; revised 30 Jan 2015; accepted 1 Feb 2015; published 11 Mar 2015

19. A. Aiello and G. S. Agarwal, "Wave-optics description of self-healing mechanism in Bessel beams," Opt. Lett. **39**(24), 6819–6822 (2014).
20. T. Aruga, "Generation of long-range nondiffracting narrow light beams," Appl. Opt. **36**(16), 3762–3768 (1997).
21. V. Belyi, A. Forbes, N. Kazak, N. Khilo, and P. Ropot, "Bessel-like beams with z-dependent cone angles," Opt. Express **18**(3), 1966–1973 (2010).
22. I. A. Litvin, N. A. Khilo, A. Forbes, and V. N. Belyi, "Intra-cavity generation of Bessel-like beams with longitudinally dependent cone angles," Opt. Express **18**(5), 4701–4708 (2010).
23. Y. Ismail, N. Khilo, V. Belyi, and A. Forbes, "Shape invariant higher-order Bessel-like beams carrying orbital angular momentum," J. Opt. **14**(8), 085703 (2012).

1. Introduction

Bessel beams (BBs) represent a class of so-called diffraction free solutions to the Helmholtz equation, and have been studied extensively [1–5] since the seminal work of Durnin *et al*. [1, 2] in the late 1980s. Experimentally it is not possible to generate such a beam (due to the infinite energy required), and so an approximation is made in the form of a Bessel function enveloped by a Gaussian profile, thereby limiting the energy carried by the field to some finite value. Such beams have been produced by many different techniques, both internal [6–8] and external [9–15] to the laser, as well as in the quantum regime with single photons and entangled states [16–18]. It is now common to create such beams with digital holograms written to spatial light modulators and much work has been done to improve the efficiency and quality of the beams produced [9–15]. Bessel beams have been topical due to their applications in optical trapping and tweezing, particle sorting, imaging, materials processing and quantum information to name but a few [1–5]. Their well-known ability to self-heal has been applied in many applications and remains a subject of ongoing study [19].

In general, the non–diffracting nature of these beams changes at the boundary of the non–diffracting region from a Bessel function (near–field profile) into a conical field with the characteristic ring–shaped intensity distribution (far–field profile), as shown in Fig. 1. This raises the question about the very nature of what it means to be non-diffracting, as ideally the Bessel profile would exist to infinity. It is possible to extend the region of non-diffracting propagation by carefully engineering the beam parameters and judicious choice of optics. For example, so-called needle beams of ultra-short pulses have been created with extended depth of focus without the need for relay optics [15].

Another approach has been to allow the cone angle of the Bessel field, γ, to decrease during propagation so that as $z\to\infty$ so $\gamma\to 0$; the Bessel-like beam that is created is shape-invariant during propagation, but at the expense of divergence in spatial extent. Such beams have been created by complex multi-element set-ups (usually three or more) with free space propagation between them [20–22]. This makes the set-up difficult to align and prohibits the option of implementing the design with a thin phase-only solution, e.g., as a diffractive optic or with spatial light modulators.

In this paper we outline a general approach to create shape invariant Bessel-like beams using single element phase-only solutions. We derive the key design equations and verify the concepts experimentally with the aid of a spatial light modulator. In contrast to previous approaches, our method is easy to implement, requires no special alignment of multiple optical elements, and provides for easy, all-digital tuneability in the output parameters of the shape invariant beam.

#227141 - $15.00 USD Received 19 Nov 2014; revised 30 Jan 2015; accepted 1 Feb 2015; published 11 Mar 2015

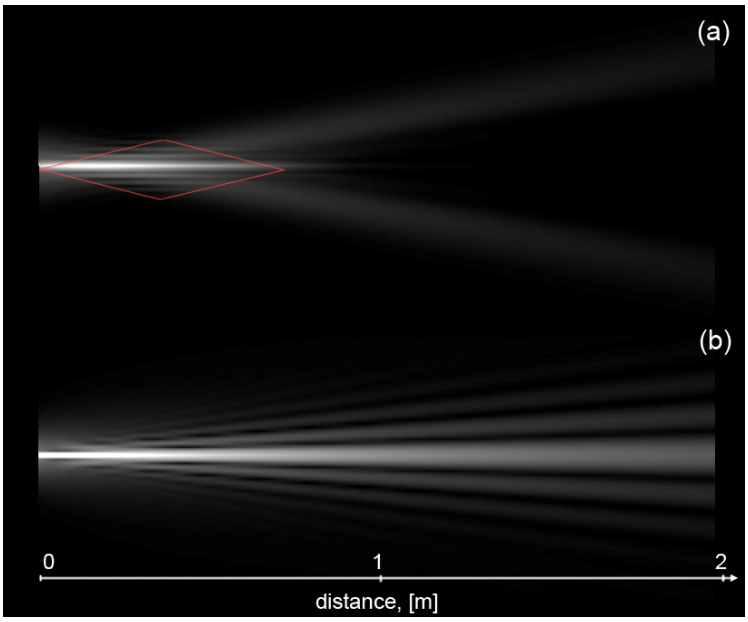

Fig. 1. Illustration of the difference between a conventional and shape-invariant Bessel beam: (a) A conventional Bessel beam is created with a digitally implemented axicon, resulting in a finite region where the Bessel field exists. (b) A novel phase screen is implemented to create a shape-invariant Bessel beam that exists in all space.

2. Theoretical approach

We wish to design a phase-only element such that the field at any transverse position along the propagation axis may be represented by a superposition of conical waves, and moreover, that the angle of arrival of the conical waves at a given plane must be identical and decrease with distance. When these conditions are satisfied the transverse field, which may be seen as the interference of these waves, will remain Bessel-like for all propagation distances. To realise such an element, let us begin with the *ansatz* that the desired phase function can be presented as a sum of two power functions so that

$$\varphi(r) = \exp\left[ik_0\left(ar^n + br^m\right)\right], \tag{1}$$

where $\varphi(r)$ is the transmission function of the phase-only element and $k_0 = 2\pi/\lambda$ is the wavenumber of the field. The problem is to find the unknown coefficients a and b given the powers n and m.

A simplified analysis of the design can be made using a geometrical optics approximation to the diffraction of the field incident on the phase-only element. The fast changing part of the integrand of the Fresnel diffraction integral is given as $ar_0^{\,n} + br_0^{\,m} + \left(r_0^{\,2}/2z\right) - \left(r_s r_0/z\right)$, where z is the distance to the screen plane, and r_0 and r_s represent the co-ordinates of a line (ray) mapped from the initial plane to the screen plane, respectively. From the method of stationary phase we can extract the mapping of rays from the initial plane of the element to some final plane (screen plane) some distance away

$$anr_0^{\,n-1} + bmr_0^{\,m-1} + \frac{r_0}{z} - \frac{r_s}{z} = 0. \tag{2}$$

Intuitively we can expect these ray positions to be similar since the interference pattern must exist to infinity. If we denote this stationary radius as r_1, then we find that our phase-only element function must satisfy

#227141 - $15.00 USD Received 19 Nov 2014; revised 30 Jan 2015; accepted 1 Feb 2015; published 11 Mar 2015

$$b = -a\frac{n}{m}(r_I)^{n-m}. \tag{3}$$

Here r_I may be interpreted as the clear aperture of the phase-only optic: any field within this radius will be converted to the desired beam in a lossless manner. Since the powers n and m are arbitrarily chosen, choice of parameter a dictates the value of b. If the phase terms in Eq. (1) are viewed as optical aberrations, then Eq. (3) provides the weighting of aberrations to produce the desired field. This simple relation allows for the optical element to be designed as a single element, hitherto not possible.

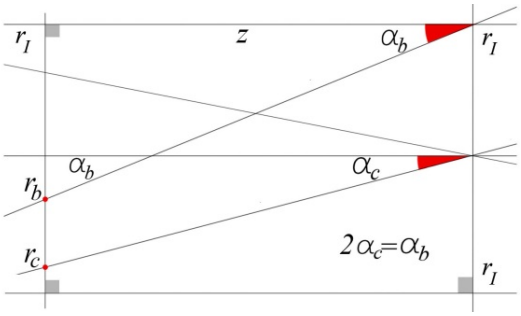

Fig. 2. We trace ray between two planes and demand that they arrive with the same cone angle at the two extreme radii (origin and at r_I).

The problem of defining the element is solved, but it is necessary to relate the element parameters to that of the desired Bessel-like field

$$u(r) \propto J_0[k\alpha_c(z)r], \tag{4}$$

where J_0 is the zero-order Bessel beam and $\alpha_c(z)$ is the cone angle which we expect to be dependent on propagation distance, z. To complete the solution, we consider the arrival angles of the rays at the screen plane at positions $r_s = 0$ (axial point) and $r_s = r_I$ (infinity point), which we denote as α_c and α_b, respectively, and assume that they originate from radial positions r_c and r_b, respectively, at the initial plane. This is illustrated in Fig. 2. We wish the rays arriving at any given plane do so at the same angle, based on Bessel Beam ray behaviour at the screen plane where all rays arrive at a given plane with the same cone angle (even if the angle differs from plane to plane), and thus a criteria for our two chosen rays must be that

$$2\alpha_c = \alpha_b. \tag{5}$$

Note that this is the extreme case: by conditioning the rays at the two extreme points on the field to meet this criterion we assume that on average all other intermediate rays will also meet this criterion. Applying Eq. (2) to these two rays, those arriving at the axial and infinity points, we easily find the following relations:

$$\begin{cases} anr_c^{\,n-1} + bmr_c^{\,m-1} + \dfrac{r_c}{z} = 0 \\ \dfrac{r_c}{z} \approx \alpha_c \end{cases}, \tag{6a}$$

$$\begin{cases} anr_b^{\,n-1} + bmr_b^{\,m-1} + \dfrac{r_b}{z} - \dfrac{r_I}{z} = 0 \\ \dfrac{r_b + r_I}{z} \approx \alpha_b \end{cases}. \tag{6b}$$

#227141 - $15.00 USD Received 19 Nov 2014; revised 30 Jan 2015; accepted 1 Feb 2015; published 11 Mar 2015

We can solve the coupled equations given by Eqs. (6) (a) and (6) (b), taking into account the relations in Eqs. (3) and (5), to find the cone angle α_c

$$\alpha_c + an\left(r_1\right)^{n-m}\left(z\alpha_c\right)^{m-1} + an\left(-r_1^{n-m}\left(-r_1+2z\alpha_c\right)^{m-1} + \left(-r_1+2z\alpha_c\right)^{n-1}\right) - an\left(z\alpha_c\right)^{n-1} = 0. \quad (7)$$

This is the general solution to finding the unknown cone angle of the Bessel-like beam given the input elements parameters of a, n and m. It is clear from Eq. (7) that the solution for the cone angle will be dependent on the propagation distance, z, as expected. By way of example, particular solutions for common optical elements are given in Table 1, namely, n = 1, m = 2 (an axicon-lens doublet), n = 2, m = 3 (aberrated lens) and n = 1, m = 3 (aberrated axicon). The solutions in the Table 1 are valid for real-valued cone angles

Table 1. Dependence of $\alpha_c^{n,m}$ angle (the cone angle of obtained Bessel beam transversal distribution) on the propagation distance z and the coefficients a and r_L

n = 1; *m* = 2	**n = 2; *m* = 3**	***n* = 1; *m* = 3**
$\alpha_c(z) = \frac{r_1 a}{az - r_1}$	$\alpha_c(z) = \frac{r_1}{12az^2}\left(1+10az \pm F(a,z)\right)$ $F(a,z) = \sqrt{1+20az+4a^2z^2}$	$\alpha_c(z) = \frac{r_1}{6az^2}\left(r_1+4az \pm G(a,w,z)\right)$ $G(a,w,z) = \sqrt{(r_1)^2+8ar_1z+4a^2z^2}$

4. Numerical simulations

This analysis can be tested using a wave optics approach, and the two results are compared in Fig. 3, where the cone angle is plotted as a function of distance. As per the design, the cone angle decreases with increasing distance. In the paraxial approximation (large separation distances) the two solutions are in very good agreement.

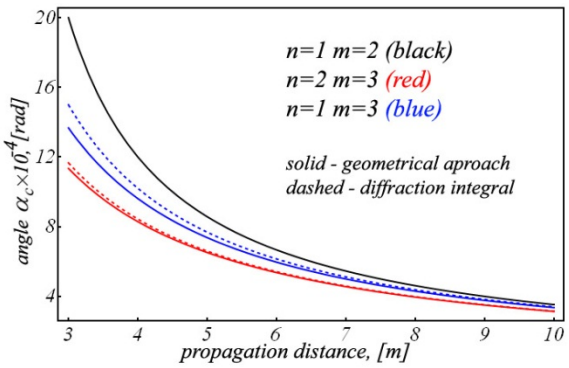

Fig. 3. Dependence of the cone angle from the geometrical optics and the wave optics approaches for different parameters of n and m. Design parameters where $a_{12} = 2 \times 10^{-3}$; $a_{23} = 1$ $a_{13} = 1.2 \times 10^{-3}$ where the subscripts refer to orders n and m, and $r_1 = 3$ mm.

As the field propagates so it maintains its shape (Bessel), all the way to the far-field. This is shown in Fig. 4 with specific cross-sections shown in Fig. 5.

#227141 - $15.00 USD Received 19 Nov 2014; revised 30 Jan 2015; accepted 1 Feb 2015; published 11 Mar 2015

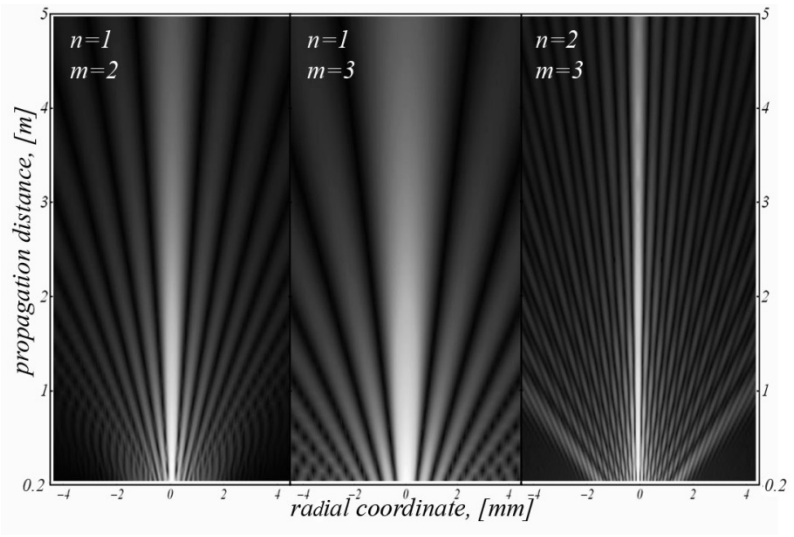

Fig. 4. Examples of the propagation characteristics of Bessel-like beams over an extended distance for r_1 = 1 mm, λ = 633 nm and (a) $a_{12} = 2.8\ 10^{-3}$, (b) $a_{13} = 8.7\ 10^{-3}$, (c) $a_{23} = 0.2$. Note that at the plane $z = 0$ the beam is a phase modulated Gaussian beam and not a Bessel function.

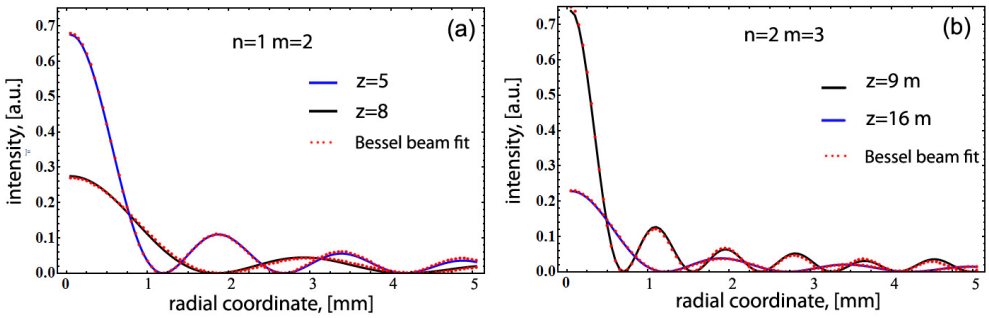

Fig. 5. The far-field intensity pattern for two examples of n and m overlaid with this is a fit of an ideal Bessel beam intensity (red). The following parameters for the initial field were used: (a) (n = 1, m = 2): $a_{12} = 2.8\ 10^{-3}$; (b) (n = 2, m = 3): a = 0.2, for r_1 = 1 mm, λ = 633 nm.

Such Bessel-like beams have some interesting properties that have been reported on previously: they are not non-diffracting but shape preserving, and may be tailored to have a higher on-axis intensity than the equivalent Gaussian beam incident on the optic. Note however that the shape is not an ideal Bessel function near the optic but becomes increasingly more so during propagation. This is evident in Fig. 5 where the Bessel fit to the beam profile is shown. However the deviation of the beam's intensity profile from a Bessel function is very small, particularly the central region of the field. Given this, and the fact that the far-field is a Bessel function and not an annular ring, the beam can be consider shape-invariant.

6. Experimental verification

To verify the theoretical results we made use of a phase-only spatial light modulator to create our shape invariant Bessel beams following Eq. (1). It should be noted that prior multi-element approaches with propagation distances between the elements prohibited such a realisation of these beams. We expanded a Gaussian laser beam from a Helium-Neon laser and modulated it following Eq. (1) using a phase-only spatial light modulator (SLM). Our SLM (HoloEye Pluto, 1080 × 1920 pixels) was calibrated for the operating wavelength to produce a maximum of 2π phase shift over the full range of grayscales in the programmed

#227141 - $15.00 USD Received 19 Nov 2014; revised 30 Jan 2015; accepted 1 Feb 2015; published 11 Mar 2015

holograms. The experimental set-up together with some example holograms are shown in Fig. 6.

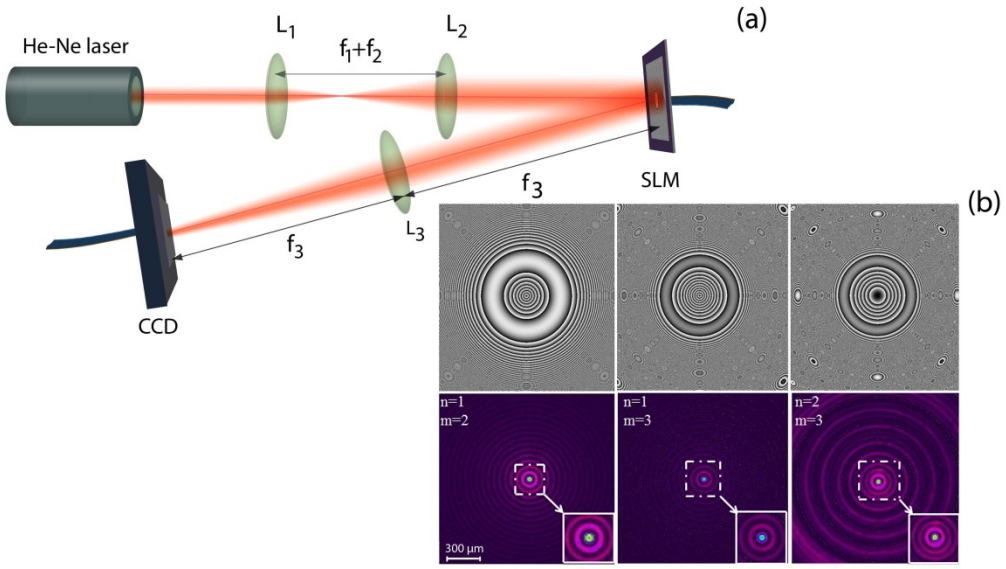

Fig. 6. (a) Schematic of the experimental set-up. (b) Some example holograms for creating Bessel-like beams and the resulting measured intensity profiles. The laser was continuous wave at a wavelength of λ = 632.8 nm. It was expanded through a 3x magnification telescope (f_1 = 100 mm and f_2 = 300 mm) and directed to the SLM. The holograms on the SLM have a depicted range from 0 (white) through to 2π (black) phase shift in 256 steps. The beam after the SLM was Fourier transformed with lens L3 (focal length f_3 = 200 mm) and the resulting beam measured on the CCD camera at the focal plane of this lens.

Figure 7 shows a comparison of theoretically predicted (top) and experimentally measured (bottom) beam profiles in both the near and far fields, the latter taken at the focal plane of a Fourier transforming lens, for the case of n = 1 and m = 2. The experimental results are in very good agreement with the theory presented earlier. Consequently we can conclude that our field is indeed shape invariant as required by theoretical analysis.

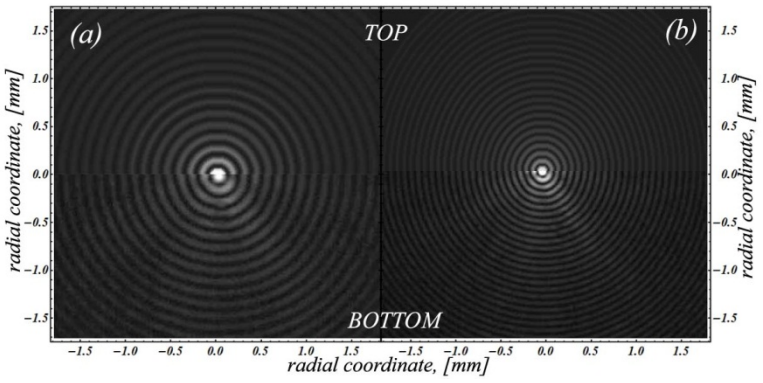

Fig. 7. (a) Near-field and (b) Far-field images of the Bessel-like beam, both theoretically (TOP) and experimentally (BOTTOM). The near-field experimental image was at a distance of 62 cm from the optical element, while the far-field was measured at the focal plane of a lens with a focal length of 40 cm.

In Fig. 8 we measure profiles for a range of propagation distances and extract the cone angle from the fit of the Bessel function to the intensity plots. The experimental results (data

#227141 - $15.00 USD Received 19 Nov 2014; revised 30 Jan 2015; accepted 1 Feb 2015; published 11 Mar 2015

points) match the theoretical curves very well for all the tested phase elements. As the theory is based on a simple geometrical approach, the results match better towards longer propagation distances. The values of k_r were extracted from fitting Bessel functions to the beam intensity cross-sections [Fig. 8(b)], and the error bars show the uncertainty in the fitting routine. There was sufficient resolution in the beam intensity measurements for the fitting.

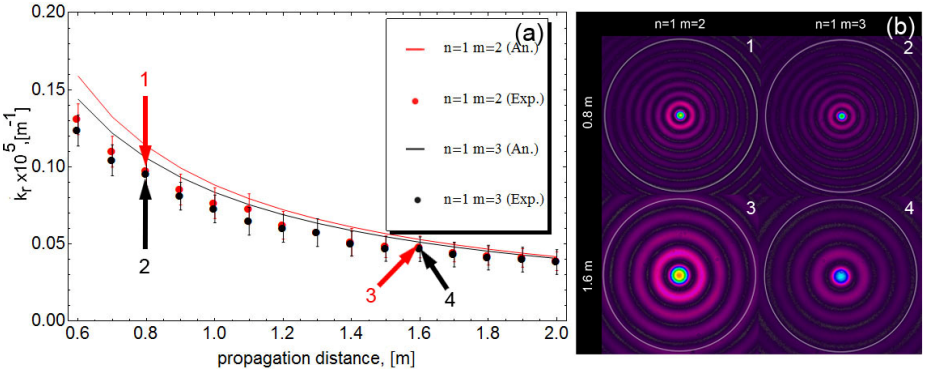

Fig. 8. (a)The experimental verification of the z-dependent radial wave number $k_r(z) = k\alpha_c(z)$, as given in Table 1 for following parameters of the phase screen and laser beam: λ = 633 nm, a = 0.01, r_1 = 0.85 mm. (b) Correspondingly obtained experimental intensity distributions at distances 0.8 m (1 and 2) and 1.6 m (3 and 4) and for n = 1, m = 2 (1 and 3) ; n = 2, m = 3 (2 and 4).

7. Discussion

One of the advantages of this approach is that the transformation from the Gaussian to the Bessel-like beam can be executed in a single phase-only device, thus making implementation on a spatial light modulator possible. Previous work in this field has considered multiple element designs with significant propagation distance between the elements. In such systems it is not possible to simply reduce the system to a thin element approximation by considering the total optical path length. As a consequence, whereas previously the properties of the Bessel-like beam could be controlled by adjusting the distance between elements, thus requiring optical realignment, here we can move within the parameter space by simply changing a hologram, requiring no optical alignment. If the hologram is reduced to that of a single axicon then the resulting beam is again the well-known Bessel beams. Our results may be extended to higher azimuthal orders, to create Bessel-like beams that carry orbital angular momentum [23], by simply modulating the holograms with an appropriate azimuthally varying phase.

There are however some limitations to these beams: the Bessel-like character is very accurate close to the center of the field and less accurate at the perimeter of the field, which can be rather complicated in structure as observed elsewhere [21]. This is also a characteristic of Bessel beams created with axicons. However, if the central region of interest is considered, then indeed the Bessel-like beam is shape invariant from a short distance after the optic through to the far field.

8. Conclusion

We have outlined a simple design approach to produce shape invariant Bessel beams from a single phase-only element, and then implemented the concept with digital holograms written to a spatial light modulator. Our experimental results confirm the theory, and thus we offer an easy to implement method for creating such beams. The advantage our single element approach will likely be apparent in compact applications such as holographic optical trapping and tweezing.

#227141 - $15.00 USD Received 19 Nov 2014; revised 30 Jan 2015; accepted 1 Feb 2015; published 11 Mar 2015